FABRICATION, OPTIMIZATION AND *IN VITRO* CYTOTOXICITY EVALUATION OF DASATINIB MONOHYDRATE-LOADED NANOPARTICLES

AJAY SAROHA[1], RAVINDER VERMA[2] , VINEET MITTAL[1] , DEEPAK KAUSHIK[1]*

[1]Department of Pharmaceutical Sciences. Maharshi Dayanand University, Rohtak-124001, India. [2]Department of Pharmaceutical Sciences, Chaudhary Bansi Lal, University, Bhiwani-127021, India
*Corresponding author: Deepak Kaushik; Email: deepkaushik1977@gmail.com

ABSTRACT

Objective: The present research aimed to formulate, optimize and evaluate dasatinib monohydrate-loaded nanoparticles using the ionic gelation method as a potential anticancer drug delivery system for enhancing its dissolution rate.

Methods: Box-Behnken design was implemented to study the effects of selected parameters chitosan concentration (X_1), Sodium Tripolyphosphate (NaTPP) concentration (X_2), and NaTPP volume (X_3) on the drug release from developed nanoparticles. Moreover, optimized formulation was evaluated for various parameters, including X-ray diffraction, differential scanning calorimetry, fourier transform infra-red, *in vitro* drug release and drug kinetics. Then, *in vitro* cytotoxicity was executed *via* MTT assay method on leukemia cell lines (RPMI 8226).

Results: The results showed optimal conditions for maximum encapsulation efficiency and minimum particle size were a low chitosan concentration, a medium NaTPP concentration, and a high NaTPP volume. The optimized batch (NP-7) demonstrated promising results with an encapsulation efficiency of 83.12±0.17%, particle size of 96.8 nm, and an *in vitro* cumulative drug release of 91.37±0.49% after 24 h. The cytotoxicity of dasatinib monohydrate was higher when administered in polymeric nanoparticles (NP-7) as compared to its pure form.

Conclusion: From this research, it can be concluded that the drug release was enhanced when dasatinib monohydrate was loaded into chitosan nanoparticles.

Keywords: Dasatinib monohydrate, Box-behnken design, Nanoparticles, Ionic gelation, *In vitro* cytotoxicity, MTT assay

INTRODUCTION

Nanoparticles (NPs) emerged in the 1970s as a Drug Delivery System (DDS) approach to improve the stability and solubility of the encapsulated molecules, promote drug delivery across cellular membranes as well as enhance drug circulation duration, improving safety and efficacy [1]. Particle sizes less than 250 nanometers are considered as nanoparticles. Nanoparticles with diameters between 10 and 200 nm have the best retention and penetration effects, making them ideal for tumor tissue accumulation [2, 3]. The drug Dasatinib Monohydrate (DSB), an aminopyrimidine derivative and tyrosine kinase inhibitor, was chosen as the model drug for this investigation. In leukemia cells, DSB inhibits Abelson Murine Leukemia (ABL1) and Breakpoint Cluster Region (BCR) and Src tyrosine kinase activity uniquely and powerfully. The US Food and Drug Administration approved this drug [4, 5]. The emergence of dasatinib and nilotinib, two second-generation TKIs, as first-line treatment for Chronic Myeloid Leukemia (CML), gave patients hope for long-term survival. As a result, transcripts encoding the BCR/ABL1 allele dropped precipitously and quickly [6, 7]. The Philadelphia (Ph) chromosome, a hematopoietic stem cell disorder known as CML, is formed when chromosomes 9 and 22 rearrange themselves. These chromosomes are themself offsprings of gene fusion between ABL1 and BCR genes. BCR-ABL1 fusion gene causes cell cycle dysregulation and the synthesis of the ABL protein, which is a constitutively active tyrosine kinase [8, 9]. Because of its high permeability and low solubility, DSB is classified as a class-II drug according to the Biopharmaceutical Classification System (BCS). Although it is suggested to be taken at large dosages, it has a short plasma half-life, lacks specificity, breaks down quickly, and is eliminated quickly [10, 11]. Dasatinib can cross the Blood-Brain Barrier (BBB) and modulate the immune system [12]. Currently, dasatinib is prescribed to patients with CML who have developed resistance to imatinib [13, 14]. N-(2-chloro-6-methyl phenyl)-2-({6-[4-(2-hydroxyethyl) piperazin-1-yl]-2-methylpyrimidin-4-yl} amino)-1, 3-thiazole-5-carboxamide [15] is its IUPAC name.

In this study, we have focused on the formulation, optimization and evaluation of nanoparticles of dasatinib monohydrate using the ionic gelation method as a potential anticancer drug delivery system.

MATERIALS AND METHODS

Material

Dasatinib monohydrate was procured from Moleculochem Private Limited, New Delhi. Bio-Gen Extract Pvt. Ltd. generously provided chitosan with a degree of deacetylation of 92.6%. (Bangalore, India). Ranbaxy Fine Chemicals Ltd. of Delhi, India, and CDH of India were the suppliers of Sodium Tripolyphosphate (NaTPP) and glacial acetic acid, respectively.

Methods

Preparation of dasatinib monohydrate nanoparticles

To develop nanoparticles, the ionic gelation approach was chosen due to its simplicity and the fact that it did not include the organic phase [16]. A solution of chitosan (0.5 to 1% w/v) in 1% v/v glacial acetic acid was used. An aqueous solution of NaTPP with 0.2 to 0.5% w/v has been prepared by dissolving drug in distilled water. The chitosan solution was supplemented with the drug at a concentration of 0.3% w/v. Then, with constant stirring, 1 drop of NaTPP solution was added to the 50 mg drug-containing chitosan solution. Ionic and electrostatic interactions between ions with opposite charges resulted in development of nanoparticulate suspension. Next, a solution was centrifuged at 18,000 rpm for 30 min at 15 °C. To eliminate any residual impurities, it was freeze-dried [17].

Optimization

The Box-Behnken Design (BBD) has been utilized to produce nanoparticles that contain dasatinib monohydrate. Three criteria were chosen, and each of them has three levels. X_1= chitosan concentration (% w/v), X_2= NaTPP concentration (% w/v), and X_3= NaTPP volume (ml) were the chosen parameters. All of the formulations keep the same drug content and chitosan volume (35 ml). The Design Expert® recommended seventeen different batches of nanoparticles loaded with dasatinib monohydrate (NP-

1 to NP-17), which were then developed and tested for the chosen response [18-22].

Evaluation of prepared nanoparticles

Particle size analysis

A laser diffractometer (Zetasizer Nano ZS90, Malvern equipment, UK) with a hydro dispersion unit was employed to measure the nanoparticle size. Diluting each sample with 2 mg of prepared nanoparticles in 5 ml of distilled water was the first step in preparing the samples for scanning at 17 runs per sample in a hydro dispersion unit. The next step was to fill the cuvettes with the diluted mixture. A cumulant diameter was then calculated by averaging the diameters of all 17 runs [23, 24].

Entrapment efficiency and loading capacity

These were assessed after the nanoparticles' extraction from the aqueous medium using ultra-centrifugation at 18,000 rpm and 15ºC for half an hour. The supernatant has been used in a UV spectrophotometer at a maximum wavelength of 294 nm to measure the quantity of free drug [25]. It was performed in triplicates. The formula shown below was used to compute these:

$$\% \, EE = \frac{\text{Total drug} - \text{Free drug X 100}}{\text{Total Drug}}$$

Attenuated total reflectance spectroscopy (ATR)

Both the drug and its excipients were subjected to ATR spectroscopy. A bench-top spectrometer was used to record the spectrum (Bruker Tensor 27, Germany). The range of 4000-400 cm^{-1} was used for the scanning of the powdered samples [26, 27].

Thermal analysis

The pure drug was subjected to a Differential Scanning Calorimetric (DSC) analysis to ascertain the component compatibility and crystalline behavior. DSC was used to conduct a DSC study (Q10 V9.9, Waters Corp., USA). The standard was indium. Scanning was performed using an empty aluminum pan and temperatures between 30 and 300 ℃ at a rate of 10 ℃ per min with a nitrogen flow rate of 60 ml/min [28, 29].

Crystallographic studies

X-ray diffraction patterns of dasatinib monohydrate powder were obtained by use of an X-ray diffractometer (AXS D5005, Bruker, Germany). Stainless steel was used as a support for the powder samples before they were exposed to Cu Kα radiation (λ = 1.54056Å) in continuous scan mode. The step size was 0.02° and the step time was 20 sec. To analyze dasatinib monohydrate and the nanoparticles, a 40 kV generator tension and a 30 mA current were used [30].

In vitro drug release studies

To study drug release *in vitro*, the modified dialysis bag method was used. The developed nanoparticles were dialyzed on a magnetic stirrer at 37±0.5 ℃ with 100 rpm in the presence of 100 ml of 0.1N HCl at a pH of 1.2. The bag was then sealed. At regular intervals, 0.1N Hydrochloric acid (HCl) was incorporated into the receptor solution to maintain the sink conditions. Quantitative evaluation of the dasatinib-containing solution was then carried out utilizing ultraviolet (UV) light at 294 nm in triplicates [31].

In vitro cytotoxicity

In Dulbecco's Modified Eagle's (DMEM) medium, a leukemia cell line RPMI 8226 from Roswell Park Memorial Institute was obtained and cultured. Centrifuged at 125 g for 5 min after removing the RPMI 8226 from its liquid nitrogen container and adding it to 9 ml of complete culture media. Following centrifugation, 10 ml of full DMEM medium was incorporated into pellets, and the supernatant was discarded. The cells were kept in an incubator with a Carbon Dioxide (CO$_2$) humidifier at a temperature of 37 ℃. Once the cell confluency reached around 80%, the cells were separated using trypsin-EDTA and then moved to two T-25 flasks. The test flask was used after the cell confluency reached around 80 to 90% [32].

MTT assay

The test agent was left out of a 96-well plate containing 200 μl of cell suspension (in full DMEM media with 10% fetal bovine serum), which was then allowed to proliferate for about 24 h. The plate included 20,000 cells per well. Following a 24 h incubation period, the test compounds have been added to the 96-well plates at the correct concentrations and left to incubate at 37 ℃ in a 5% CO$_2$ environment for another 48 h. Once the incubation time was over, the plates were taken out of the incubator. The wasted medium was then drained and MTT reagent was added until it reached a final concentration of 0.5 mg/ml, using a 0.2 μm filter that had been sterilized. To keep the plates from getting any light, they were enclosed with aluminum foil and put in an incubator for three hours. Following the incubation period, 100 μl of dimethyl sulfoxide was added after the MTT reagent had been withdrawn. Spectrophotometer readings were taken at 570 nm using a TecanTM Infinite 200 Pro. It was performed in triplicates [33].

RESULTS AND DISCUSSION

To develop dasatinib-loaded chitosan nanoparticles, the positive charge on chitosan and the negative charge on NaTPP interacted electrostatically during the ionic gelation process. Box-Behnken Design was implemented. Three parameters—concentration of chitosan, the concentration of NaTPP, and volume of NaTPP—each of which had three possible values (-1, 0,+1) were selected. Suggested seventeen nanoparticle formulations loaded with dasatinib were developed. Using the Design Expert software (version 8.0.7.1), we analyzed the particle sizes statistically. Table 1 shows the results of particle size of dasatinib monohydrate-loaded chitosan nanoparticles.

Table 1: Formulation suggested by design expert and their characterization (NP1 to NP17)

Batch No.	X1 (Conc. of chitosan)	X2 (Conc. Of NaTPP)	X3 (Vol. of NaTPP)	Particle size (nm)	EE (%)*
NP1	200	100	50	281.8	74.51±1.21
NP2	400	100	50	343.6	76.45±1.37
NP3	200	300	50	370.1	67.19±0.89
NP4	400	300	50	356.3	72.54±1.10
NP5	200	200	25	310.4	55.31±0.69
NP6	400	200	25	293.2	64.23±0.93
NP7	200	200	75	96.8	83.12±1.42
NP8	400	200	75	245.9	78.36±1.39
NP9	300	100	25	198.6	69.27±0.99
NP10	300	300	25	382.1	76.97±1.32
NP11	300	100	75	312.7	51.66±0.61
NP12	300	300	75	150.3	81.49±1.42
NP13	300	200	50	360.2	68.18±0.90
NP14	300	200	50	308.4	65.41±0.81
NP15	300	200	50	308.3	69.38±1.01
NP16	300	200	50	314.6	66.07±0.96
NP17	300	200	50	334.5	71.22±1.05

Abbreviations: Conc.-Concentration, Vol.-Volume. *All results are given as mean±SEM (n=3).

Particle size

A size distribution of particles ranging from 96.8 nm to 382.1 nm was observed (table 1). The smallest particles were produced by increasing the NaTPP volume, decreasing the chitosan content, and maintaining a medium concentration of NaTPP. Perovskite size peaked at medium chitosan concentration, high NaTPP concentration, and low NaTPP volume. NP-7 formulation showed a particle size of 96.8 nm. They were spherical, with uniform internal distribution and good dispersion [34].

Analysis of Variance (ANOVA) was used to examine the mathematical model's fit and significance to this estimate. The responses demonstrated in fig. 1, the findings of the particle size investigation, were fitted using the response surface quadratic model.

One such mathematical expression for the model that predicts particle size (Y_1) using multiple linear regression is:

$$Y_1 = 325.20 + 22.49X_1 + 15.26X_2 - 47.32X_3 - 18.90X_1X_2 + 41.57X_1X_3 - 86.47X_2X_3 - 5.80X_1^2 + 18.55X_2^2 - 82.83X_3^2$$

Where Y_1 = Particle size, X_1 = Concentration of chitosan, X_2 = Concentration of NaTPP, X_3 = Volume of NaTPP

The positive coefficients indicate that size is positively impacted. In contrast, negative coefficients before independent variables signify an unfavorable impact on size [35]. To examine the mathematical model's fit and relevance in estimating particle size, ANOVA has been utilized, as given in table 2.

Table 2: Results of ANOVA for particle size

ANOVA	Degree of freedom	Sum of squares	mean **square**	F-value	F-significance"
Regression	9	92187.07	10243.01	11.50	Significant
Residual	7	6232.88	890.41	-	-
Total	16	98419.95			

When comparing the regression and residual means squares, an F-test was used. There is statistical evidence of a substantial regression (F = 11.50). Particle size response surfaces based on the predicted model are therefore possible. Both the 3 Dimesional (3D) surface model and the contour model graphs about particle size are shown in fig. 1.
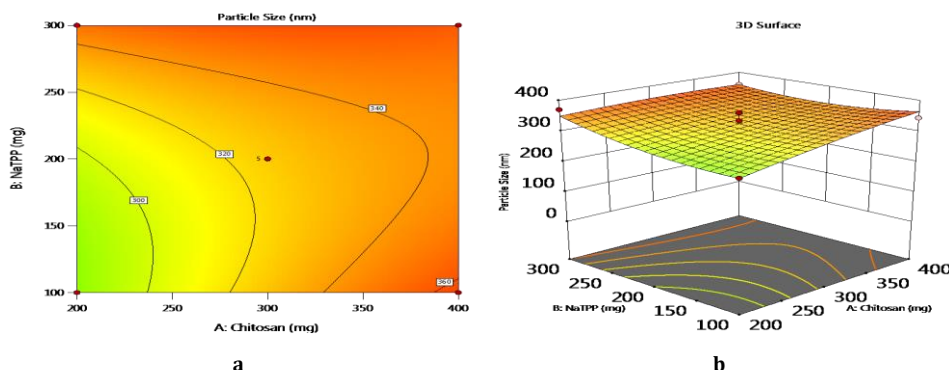

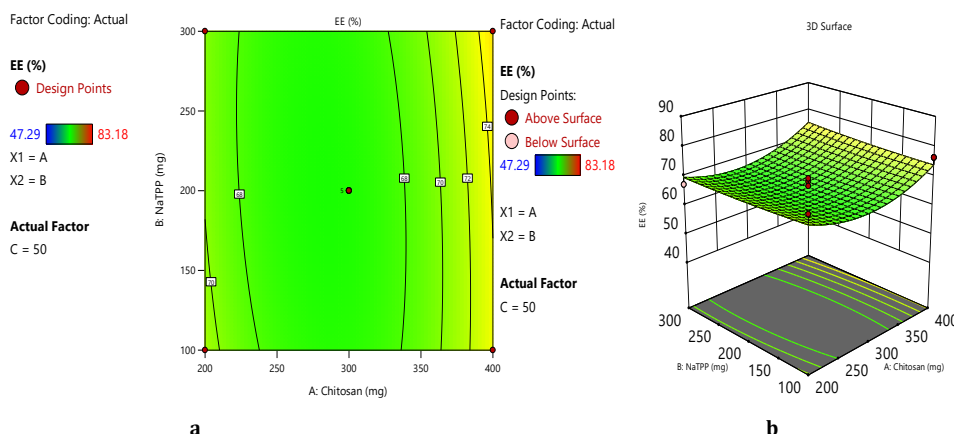**Fig. 1: (a) 2D contour model graph and (b) 3D surface model graph for particle size**

Fig. 2: (a) 2D contour model graph and (b) 3D surface model graph for % EE

% Entrapment efficiency (% EE)

% EE ranging from 51.66 to 83.2% was observed as shown in table 1. The highest %EE was produced by the medium NaTPP volume, the lowest the chitosan content, and a medium concentration of NaTPP. ANOVA was used to examine the mathematical model's fit

and significance for this estimate. To get the response shown in fig. 2, the findings of the %EE investigation were fitted using the response surface quadratic model.

One such mathematical expression for the model that predicts %EE using multiple linear regressions is:

$Y_2 = +66.30++2.15X_1+0.0500X_2+12.18X_3+0.66X_1X_2-3.58X_1X_3-1.03X_2X_3+5.72X_1^2+0.4565X_2^2-4.27X_3^2$

Where Y_2 = %EE, X_1 = Concentration of chitosan, X_2 = Concentration of NaTPP, X_3 = Volume of NaTPP

When comparing the regression and residual means squares, an F-test was used. There is statistical evidence of a substantial regression (F = 8.51), indicating the linear response surface and quadratic model was significant as mentioned in table 2 [35]. % EE response surfaces based on the predicted model are therefore possible. Both the 3D surface model and the contour model graphs about % EE are shown in fig. 2 and the desirability index is shown in fig. 3. Based on coded equations and desirability index, NP-7 was found to be an optimized formulation that was further evaluated for various parameters.

Attenuated total reflectance spectroscopy (ATR)

Both the pure drug (DSB) and DSB loaded nanoparticles had their spectra recorded, as seen in fig. 4. The pure drug's ATR spectrum showed characteristic peaks at 1300.22 cm⁻¹ for C-C stretching, 1677.33 cm⁻¹ for C=C stretching, 1211.34 cm⁻¹ for C-N stretching, 3408.61 cm⁻¹ for N-H stretching, 2991.68 cm⁻¹ for aromatic C-H stretching, 1047.33 cm⁻¹ for aromatic C-H bending and 681.33 cm⁻¹ C-Cl stretching as shown in table 3 which proved the correct structure of dasatinib [36]. When comparing the ATR spectra of the pure drug with the formulation, there was no evidence of altered functional peaks, overlapping distinctive peaks, or the emergence of completely new peaks that confirmed that there was no chemical incompatibility among selected excipients and drug.
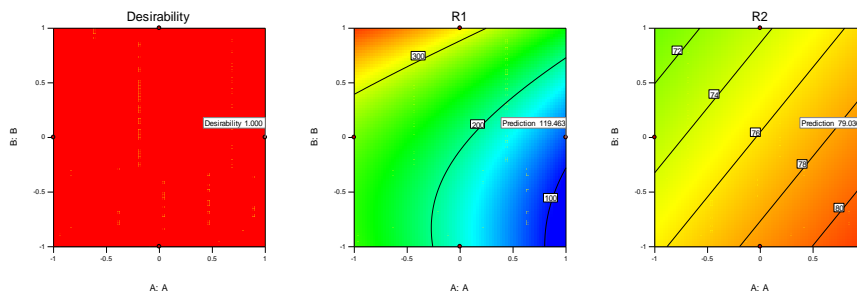

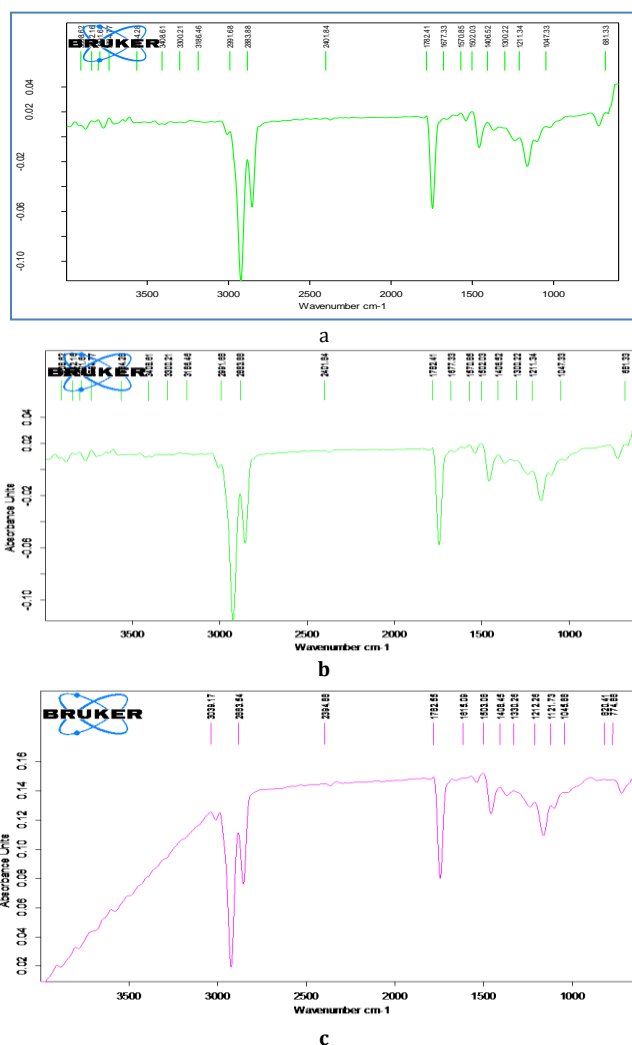**Fig. 3: Desirability index for optimized formulation**

Fig. 4: ATR spectrum of (a) dasatinib monohydrate, and (b) physical mixture and NP-7

Table 3: ATR compatibility studies of drug and excipients

Groups	Reported values	Observed values for pure drug (cm⁻¹)	Observed values for drug and excipients (cm⁻¹)
C-C stretching	1300-400	1300.22 cm⁻¹	1328.07
C=C stretching	1700-1600	1677.33 cm⁻¹	1669.89
C-N stretching	1080-1360	1211.34 cm⁻¹	1211.02
N-H stretching	3600-3310	3408.61 cm⁻¹	3611.06
Aromatic C-H stretching	3200-3000	2991.68 cm⁻¹	2989.26
Aromatic C-H bending	1000-675	1047.33 cm⁻¹	1061.79
C-Cl stretching	600-800	681.33 cm⁻¹	657.15

Differential scanning calorimetry (DSC) analysis

Fig. 5(a) shows that dasatinib has a single strong endothermic peak at 283.45 °C, which was about the same as its melting point. The physical combination tested positive for dasatinib monohydrate and polymer by DSC as shown in fig. 5(b). NP-7 did not exhibit endothermic peak as shown in fig. 5(c). This is because, when nanoparticles were formed, the drug was either dissolved in a polymer matrix or distributed in an amorphous form.
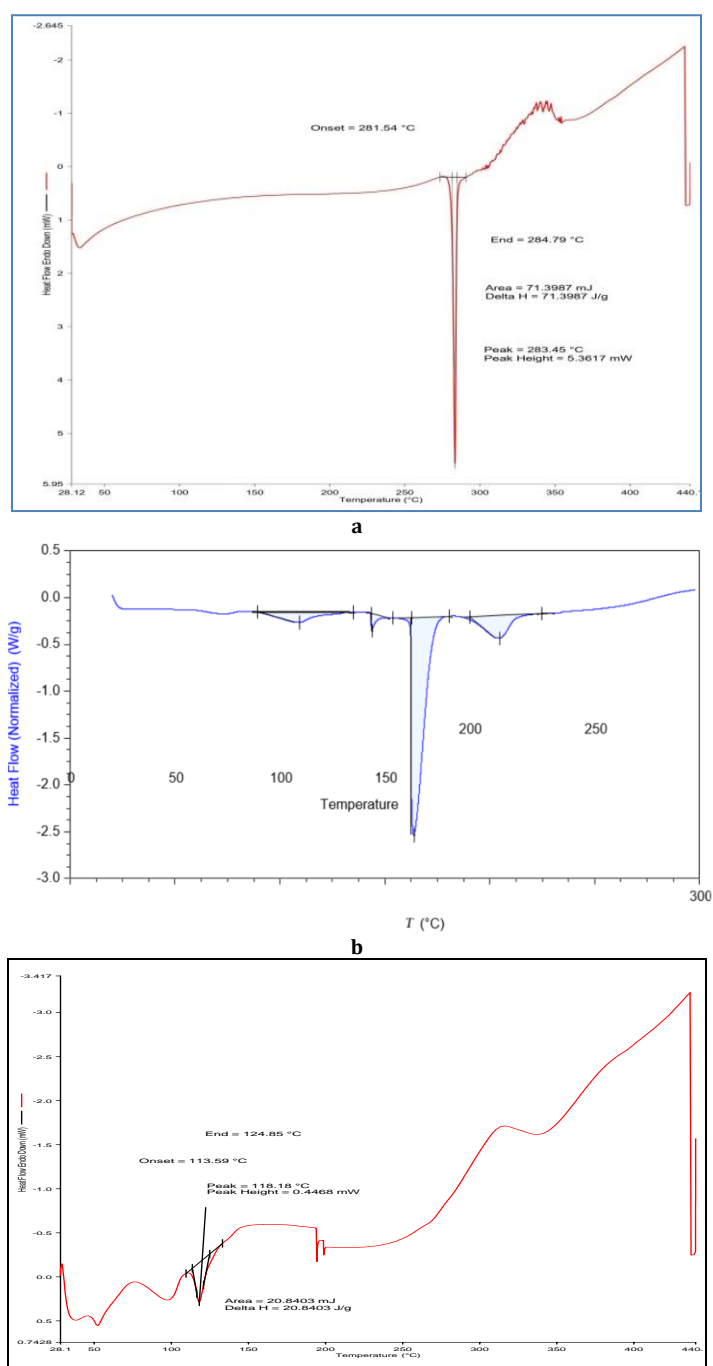

a

b

Fig. 5: DSC spectrum of (a) dasatinib monohydrate, (b) physical mixture and (c) NP-7 formulation

X-ray diffraction (XRD)

The dissolution rate of NPs is not only governed by particle size of the drug but also by its crystalline/amorphous state. Usually, dissolution rate of amorphous drugs is faster than that of crystalline. In addition, drug amorphization can also result in greater saturation solubility. To assess state of drugs upon nanonization, we analyzed their diffraction pattern by PXRD [37]. Fig. 6(a) shows that the DSB's XRD spectra revealed its crystalline form with distinct and moderately strong peaks at 2θ angles of

12.33°, 13.15°, 13.17°, 13.72°, 16.17°, and 24.36°. XRD pattern for the NP-7 formulation is shown in fig. 6(b). According to the diffraction patterns, DSB lost some of its crystalline structure and became more amorphous. This is supported by the presence of many large diffuse peaks. The appearance of the new peaks suggests that this drug underwent changes during nanonization, which may have led to the formation of a different polymorph [37]. Nanoparticle spectrum exhibited broad diffuse peaks, which suggest that the crystalline nature of the DSB was decreased and converted into amorphous nature [38].
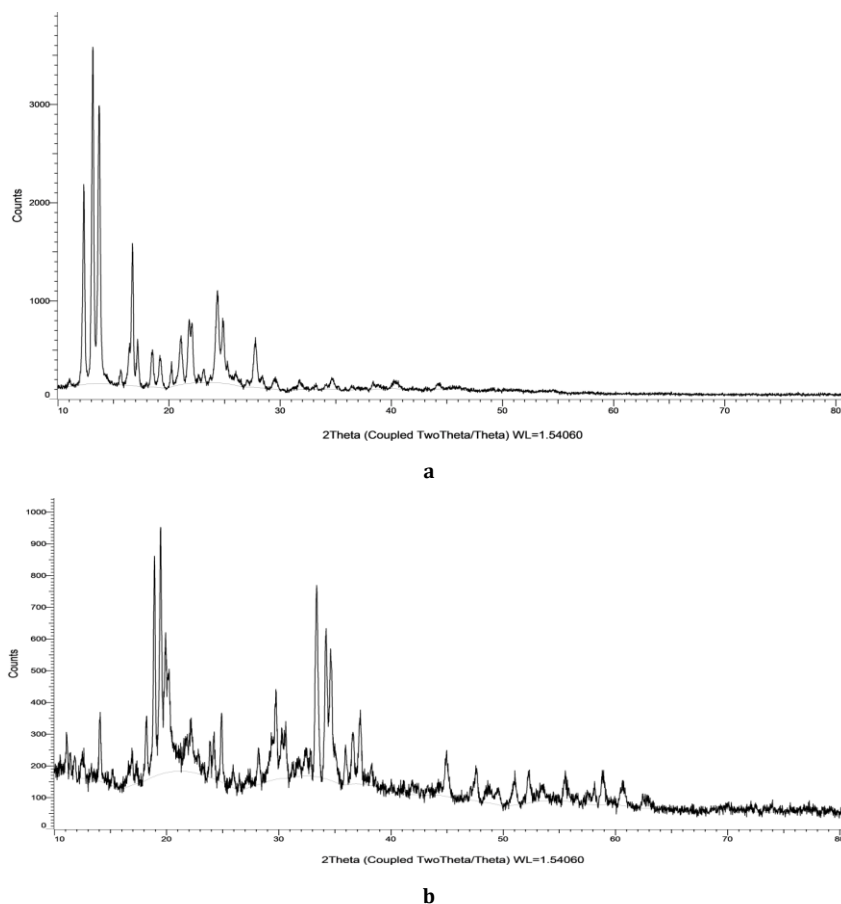

a

b
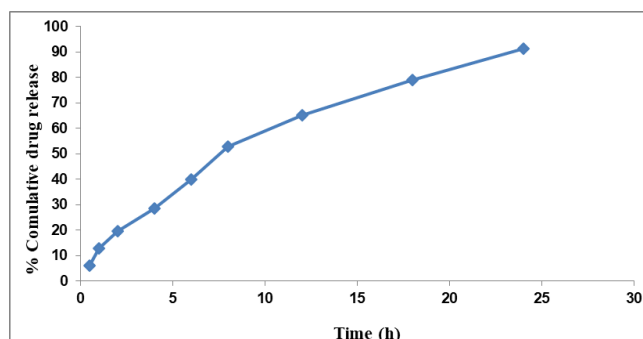
Fig. 6: XRD Spectrum of (a) dasatinib monohydrate and (b) NP 7

Fig. 7: *In vitro* drug release profile of NP-7 in 0.1N HCl

***In vitro* drug release studies**

When the characteristics NPs were revealed, we need to verify the release of DSB. This is one of the main parameters of the carrier [39-40]. Formulation NP-7 was chosen for further *in vitro* drug release investigation due to its small particle size and good entrapment effectiveness. There was a 91.37% cumulative release of the drug

from optimized formulation (NP-7) after 24 h in 0.1N HCl at pH 1.2. Fig. 7 shows the results of *in vitro* drug release investigation.

Release kinetics

The optimized batch NP-7 showed high correlation coefficient (R^2) values on the drug release mechanism as well as kinetics. Different

kinetics models have been fitted to the *in vitro* drug release data using DD Solver 1.0. Table 4 shows that the zero-order, first-order, Higuchi, and Korsmeyer-Peppas models have R^2 values of 0.940, 0.985, 0.988, and 0.990, respectively. According to the Korsmeyer-Peppas model, the drug release mechanism from the nanoparticles was determined to be non-fickian diffusion because of its highest correlation value.

Table 4: Correlation coefficients for drug release kinetics

Release model	Correlation coefficients (R^2)
Zero Order	0.947
Higuchi release model	0.985
First Order	0.988
Korsmeyer-peppas model	0.990

In vitro cytotoxicity study

In order to detect the antitumor activity of nanoparticles and pure drug, leukemia cell line RPMI 8226 were selected. The cytotoxic activity of dasatinib monohydrate, both in its pure form and as a loaded chitosan nanoparticle was investigated. Because of its small particles and high entrapment efficiency, the NP-7 formulation was chosen for cytotoxicity investigation. Particle size has a significant impact on absorption of drug in cancerous cell, and a zeta potential value increases cytotoxicity by interacting more strongly with tumorous cell [2]. Particle size and zeta potential may be related to the cytotoxicity of dasatinib monohydrate-loaded chitosan nanoparticles. The cytotoxicity of dasatinib monohydrate was higher when administered in polymeric nanoparticles (NP-7) as compared to its pure form. The delayed release rate of dasatinib monohydrate-loaded chitosan nanoparticles may be responsible for their increased cytotoxicity. When comparing free dasatinib monohydrate and NP-7, the IC_{50} value was found to be 40.93 μg/ml and 42.18 μg/ml, respectively as shown in fig. 8 and table 5. It is suggested that developed nanoparticles have more significant cytotoxic effects on these cell lines. For dasatinib, cell viability significantly decreased with an increase in drug-loaded nanoparticles [39]. The reason was that nanoparticles increased the water solubility and targeting of drugs, increased the concentration of drugs in cells, and showed a stronger inhibitory effect on cells. The IC_{50} value reflected the same results [41]. These results revealed that nanoparticle formulation was more effective at cytotoxicity than pure drug.
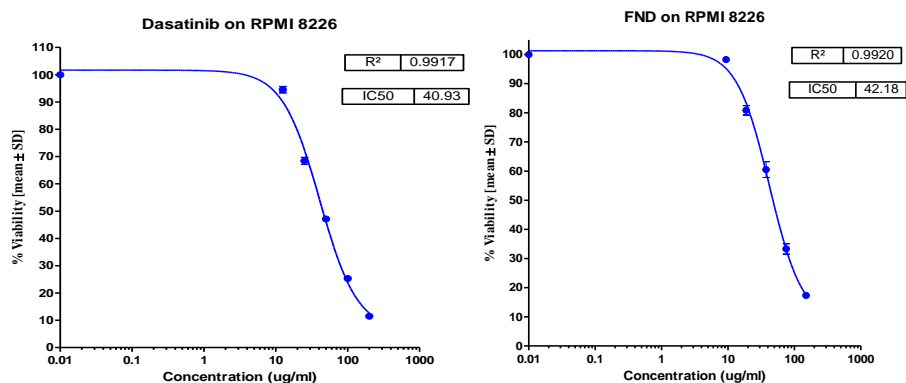

Fig. 8: % viability graph of pure dasatinib monohydrate and prepared nanoparticles (NP-7), All results are given as mean (n=3)

Table 5: Results of IC_{50} value for pure drug and nanoformulation (n=3)

S. No.	Compound	IC_{50} value (μg/ml)
1.	Pure drug	40.93±0.12
2.	NP-7	42.18±0.18

All results are given as mean±SEM (n=3).

CONCLUSION

In this study, we have successfully fabricated a safe and efficient drug delivery system that can achieve a slow release of drug and target tumor cell lines. The nanosystem takes dasatinib as part of the carrier, effectively improving dissolution rate of the dasatinib monohydrate using ionic gelation method. Both entrapment and loading efficiency were high for the developed dasatinib monohydrate nanoparticles. Drug release was influenced by chitosan molecular weight and NaTPP matrix cross-linking agent. The developed nanoparticles showed good control release for 24 h in the treatment of CML. At low concentrations of polymer (chitosan), mid-level concentrations of NaTPP and high levels of NaTPP volume, the response surface quadratic model best fit the ANOVA on particle size, which revealed that the prepared nanoparticles have the smallest size. Based on coded equations and desirability index, NP-7 was found to be an optimized formulation.

The release of the drug from the nanoparticles followed a non-fiction diffusion process because of its highest correlation value of 0.990. When comparing pure dasatinib monohydrate and NP-7, the IC_{50} value was found to be 40.93 μg/ml and 42.18 μg/ml, respectively. Particle size showed significant impact on absorption of drug in cancerous cell, and a zeta potential value increaseed cytotoxicity by interacting more strongly with tumorous cell. Particle size and %EE is related to the cytotoxicity of dasatinib monohydrate-loaded chitosan nanoparticles. This study provides an effective strategy for the design of nanomedicines with high selectivity and improved antitumor effects of dasatinib.

AUTHORS CONTRIBUTIONS

Ajay Saroha: Writing-Original Draft Preparation, Conceptualization; Ravinder Verma: Software, Writing-Review and Editing, Data Curation; Vineet Mittal: Conceptualization; Deepak Kaushik: Conceptualization, Supervision. All authors have read and agreed to publish the manuscript.

CONFLICT OF INTERESTS

Declared none

REFERENCES

1. Moya Lopez C, Juan A, Donizeti M, Valcarcel J, Vazquez JA, Solano E. Multifunctional PLA/gelatin bionanocomposites for tailored drug delivery systems. Pharmaceutics. 2022 May 27;14(6):1138. doi: 10.3390/pharmaceutics14061138, PMID 35745711.

2. Javaid MH, Chen N, Yasin MU, Fan X, Neelam A, Rehman M. Green-synthesized lignin nanoparticles enhance Zea mays resilience to salt stress by improving antioxidant metabolism and mitigating ultrastructural damage. Chemosphere. 2024;359:142337. doi: 10.1016/j.chemosphere.2024.142337, PMID 38754490.

3. Rani A, Verma R, Mittal V, Bhatt S, Kumar M, Tiwari A. Formulation development and optimization of rosuvastatin loaded nanosuspension for enhancing dissolution rate. Curr Drug Ther. 2023;18(1):75-87. doi: 10.2174/1574885517666220822104652.

4. Mian AA, Rafiei A, Haberbosch I, Zeifman A, Titov I, Stroylov V. PF-114, a potent and selective inhibitor of native and mutated BCR/ABL is active against philadelphia chromosome-positive (Ph+) leukemias harboring the T315I mutation. Leukemia. 2015;29(5):1104-14. doi: 10.1038/leu.2014.326, PMID 25394714.

5. Obr A, Roselova P, Grebenova D, Kuzelova K. Real-time analysis of imatinib and dasatinib-induced effects on chronic myelogenous leukemia cell interaction with fibronectin. Plos One. 2014;9(9):e107367. doi: 10.1371/journal.pone.0107367, PMID 25198091.

6. Adeola HA, Bano A, Vats R, Vashishtha A, Verma D, Kaushik D. Bioactive compounds and their libraries: an insight into prospective phytotherapeutics approach for oral mucocutaneous cancers. Biomed Pharmacother. 2021;141:111809. doi: 10.1016/j.biopha.2021.111809, PMID 34144454.

7. Garcia Gutierrez V, Hernandez Boluda JC. Tyrosine kinase inhibitors available for chronic myeloid leukemia: efficacy and safety. Front Oncol. 2019;9:603. doi: 10.3389/fonc.2019.00603, PMID 31334123.

8. Daley GQ, Van Etten RA, Baltimore D. Induction of chronic myelogenous leukemia in mice by the P210bcr/abl gene of the Philadelphia chromosome. Science. 1990;247(4944):824-30. doi: 10.1126/science.2406902, PMID 2406902.

9. Heisterkamp N, Groffen J, Stephenson JR, Spurr NK, Goodfellow PN, Solomon E. Chromosomal localization of human cellular homologues of two viral oncogenes. Nature. 1982;299(5885):747-9. doi: 10.1038/299747a0, PMID 7121606.

10. Bertrand N, Wu J, Xu X, Kamaly N, Farokhzad OC. Cancer nanotechnology: the impact of passive and active targeting in the era of modern cancer biology. Adv Drug Deliv Rev. 2014;66:2-25. doi: 10.1016/j.addr.2013.11.009, PMID 24270007.

11. Jain RK, Stylianopoulos T. Delivering nanomedicine to solid tumors. Nat Rev Clin Oncol. 2010;7(11):653-64. doi: 10.1038/nrclinonc.2010.139, PMID 20838415.

12. Korashy HM, Rahman AF, Kassem MG. Dasatinib. Profiles Drug Subst Excip Relat Methodol. 2014;39:205-37.

13. Haslam S. Dasatinib: the emerging evidence of its potential in the treatment of chronic myeloid leukemia. Core Evid. 2005;1(1):1-12. PMID 22496672.

14. Kantarjian H, Pasquini R, Hamerschlak N, Rousselot P, Holowiecki J, Jootar S. Dasatinib or high-dose imatinib for chronic-phase chronic myeloid leukemia after failure of first-line imatinib: a randomized phase 2 trial. Blood. 2007;109(12):5143-50. doi: 10.1182/blood-2006-11-056028, PMID 17317857.

15. Madur S, Matole V, Kalshetti M. UV–visible spectrophotometric method development and validation of dasatinib in bulk and solid dosage form. Int J Curr Pharm Sci. 2020;12(4):90-3. doi: 10.22159/ijcpr.2020v12i4.39089.

16. Idacahyati K, Wulandari WT, Indra FG. Synthesis of encapsulated chromolaena odorata leaf extract in chitosan nanoparticle by using ionic gelation method and its antioxidant activity. Int J App Pharm. 2021;13(4):112-5. doi: 10.22159/ijap.2021.v13s4.43828.

17. Nagaverma BV, Yadav HK, Vasudha LS, Shivakumar HG. Different techniques for preparation of polymeric nanoparticles. Asian J Pharm Clin Res. 2012;1:16-23.

18. Bezerra MA, Santelli RE, Oliveira EP, Villar LS, Escaleira LA. Response surface methodology (RSM) as a tool for optimization in analytical chemistry. Talanta. 2008;76(5):965-77. doi: 10.1016/j.talanta.2008.05.019, PMID 18761143.

19. Kaushik R, Verma R, Budhwar V, Kaushik D. Investigation of solid dispersion approach for the improvement of pharmaceutical characteristics of telmisartan using a central composite design. Int J App Pharm. 2023;15(5):245-54. doi: 10.22159/ijap.2023v15i5.47968.

20. Devi S, Kumar S, Verma V, Kaushik D, Verma R, Bhatia M. Enhancement of ketoprofen dissolution rate by the liquisolid technique: optimization and *in vitro* and *in vivo* investigations. Drug Deliv Transl Res. 2022;12(11):2693-707. doi: 10.1007/s13346-022-01120-x, PMID 35178670.

21. Decaestecker TN, Lambert WE, Van Peteghem CH, Deforce D, Van Bocxlaer JF. Optimization of solid-phase extraction for a liquid chromatographic-tandem mass spectrometric general unknown screening procedure by means of computational techniques. J Chromatogr A. 2004;1056(1-2):57-65. doi: 10.1016/j.chroma.2004.06.010, PMID 15595533.

22. Bharti Sharma J, Bhatt S, Tiwari A, Tiwari V, Kumar M, Verma R. Statistical optimization of tetrahydrocurcumin loaded solid lipid nanoparticles using box behnken design in the management of streptozotocin-induced diabetes mellitus. Saudi Pharm J. 2023 Sep;31(9):101727. doi: 10.1016/j.jsps.2023.101727, PMID 37638219.

23. Verma R, Mittal V, Kaushik D. Quality-based design approach for improving oral bioavailability of valsartan loaded smedds and study of impact of lipolysis on the drug diffusion. Drug Deliv Lett. 2018;8(2):130-9. doi: 10.2174/2210303108666180313141956.

24. Begum MY, Gudipati PR. Formulation and evaluation of dasatinib-loaded solid lipid nanoparticles. Int J Pharm Pharm Sci. 2018;10(12):14-20. doi: 10.22159/ijpps.2018v10i12.27567.

25. Elzoghby AO, Samy WM, Elgindy NA. Novel spray-dried genipin-crosslinked casein nanoparticles for prolonged release of alfuzosin hydrochloride. Pharm Res. 2013;30(2):512-22. doi: 10.1007/s11095-012-0897-z, PMID 23135815.

26. Setiawan F, Rusdiana T, Gozali D, Nurdianti L, Idacahyati K, Wulandari WT. Formulation and characterization of zeaxanthin nanoemulsion radiance serum as an antioxidant. Int J App Pharm. 2022;14(4):116-20. doi: 10.22159/ijap.2022.v14s4.PP27.

27. Pillai VK. Meet our editorial board member. ACCTRA. 2018;5(1):1. doi: 10.2174/2213476X0501180528083213.

28. Sinha S, Thapa S, Singh S, Dutt R, Verma R, Pandey P. Development of biocompatible nanoparticles of tizanidine hydrochloride in orodispersible films: *in vitro* characterization, *ex vivo* permeation, and cytotoxic study on carcinoma cells. Curr Drug Deliv. 2022;19(10):1061-72. doi: 10.2174/1567201819666220321111338, PMID 35319369.

29. Trapani A, Esteban MA, Curci F, Manno DE, Serra A, Fracchiolla G. Solid lipid nanoparticles administering antioxidant grape seed-derived polyphenol compounds: a potential application in aquaculture. Molecules. 2022;27(2):344. doi: 10.3390/molecules27020344, PMID 35056658.

30. Singh K, Singh A, Mishra A. Synthesis, characterization and *in vitro* release profile of gentamicin loaded chitosan nanoparticle. Int J Pharm Technol. 2016;9(10):29189-98.

31. Adena SK, Matte KV, Kosuru R. Formulation, optimization and *in vitro* characterization of dasatinib loaded polymeric nanocarriers to extend the release of the model drug. Int J Appl Pharm. 2021;13(5):318-30.

32. Alley MC, Scudiero DA, Monks A, Hursey ML, Czerwinski MJ, Fine DL. Feasibility of drug screening with panels of human tumor cell lines using a microculture tetrazolium assay. Cancer Res. 1988;48(3):589-601. PMID 3335022.

33. Noor F, Niklas J, Müller Vieira U, Heinzle E. An integrated approach to improved toxicity prediction for the safety assessment during preclinical drug development using Hep G2 cells. Toxicol Appl Pharmacol. 2009;237(2):221-31. doi: 10.1016/j.taap.2009.03.011, PMID 19332084.

34. Niza E, Nieto Jimenez C, Noblejas Lopez MD, Bravo I, Castro Osma JA, Cruz Martinez F. Poly(cyclohexene phthalate) nanoparticles for controlled dasatinib delivery in breast cancer

therapy. Nanomaterials (Basel). 2019 Aug 27;9(9):1208. doi: 10.3390/nano9091208, PMID 31461998.

35. M, Neekhra S, Swarnkar S, Gupta P, Gupta D, Khunteta A. Dasatinib and hesperidin loaded nanoformulation and preclinical evaluation for anticancer activity. IJPQA. 2020;14(3):579-86. doi: 10.25258/ijpqa.14.3.20.

36. Yang L, Xu J, Xie Z, Song F, Wang X, Tang R. Carrier-free prodrug nanoparticles based on dasatinib and cisplatin for efficient antitumor *in vivo*. Asian J Pharm Sci. 2021 Nov;16(6):762-71. doi: 10.1016/j.ajps.2021.08.001, PMID 35027952.

37. Arzi RS, Kay A, Raychman Y, Sosnik A. Excipient-free pure drug nanoparticles fabricated by microfluidic hydrodynamic focusing. Pharmaceutics. 2021 Apr 10;13(4):529. doi: 10.3390/pharmaceutics13040529, PMID 33920184.

38. Reddy Adena SK, Matte KV, Kosuru R. Formulation, optimization, and *in vitro* characterization of dasatinib loaded polymeric nanocarriers to extend the release of the model drug.

Int J App Pharm. 2021;13(5):318-30. doi: 10.22159/ijap.2021v13i5.41995.

39. Zhang Y, Zeng X, Wang H, Fan R, Hu Y, Hu X. Dasatinib self-assembled nanoparticles decorated with hyaluronic acid for targeted treatment of tumors to overcome multidrug resistance. Drug Deliv. 2021 Dec;28(1):670-9. doi: 10.1080/10717544.2021.1905751, PMID 33792436.

40. Verma R, Kaushik D. Development, optimization, characterization and impact of *in vitro* lipolysis on drug release of telmisartan loaded SMEDDS. Drug Deliv Lett. 2019;9(4):330-40. doi: 10.2174/2210303109666190614120556.

41. Zeng X, Wang H, Zhang Y, Xu X, Yuan X, Li J. pH-responsive hyaluronic acid nanoparticles for enhanced triple-negative breast cancer therapy. Int J Nanomedicine. 2022 Mar 25;17:1437-57. doi: 10.2147/IJN.S360500, PMID 35369031.